International Journal of Applied Pharmaceutics

ISSN- 0975-7058 Vol 10, Issue 5, 2018

Original Article

SPRAY DRIED LACTOSE BASED PRONIOSOMES AS STABLE PROVESICULAR DRUG DELIVERY CARRIERS: SCREENING, FORMULATION, AND PHYSICOCHEMICAL CHARACTERIZATION

ALI NASR[1,2*], MONA QUSHAWY[1,3], SHADY SWIDAN[4]

[1]Department of Pharmaceutics, Faculty of Pharmacy, Sinai University, Alarish, Egypt, [2]Department of Pharmaceutics, Faculty of Pharmacy, Port Said University, Port Said, Egypt, [3]Department of Pharmaceutics, Faculty of Pharmacy, University of Tabuk, Tabuk, Saudi Arabia, [4]Department of Pharmaceutics, Faculty of Pharmacy, The British University in Egypt, Cairo, Egypt
Email: ali.nasr@su.edu.eg

Received: 05 Jun 2018, Revised and Accepted: 16 Jul 2018

ABSTRACT

Objective: In the present investigation efforts were considered to optimize the different conditions for the preparation of spray dried lactose based proniosomes. The aim of this research was to investigate the feasibility of proniosomes as stable precursors for the development of niosomes as oral drug delivery system for poorly water-soluble drugs.

Methods: A total of twenty-eight plain proniosomal formulae were prepared with various surfactant-cholesterol loading ratios in each formula using spray dried lactose as a carrier. Span 20, 40, 60 and 80 were used in various molar ratios with cholesterol. Different evaluation techniques were performed to study the performance of the prepared proniosomes. The micromeritic properties of the prepared proniosomes were analyzed. The reconstituted niosomes were further evaluated for morphological characterization using transmission electron microscope (TEM), particle size analysis, zeta potential, and polydispersity index (PDI). Finally, selected proniosomal formulae were tested for stability study.

Results: The proniosomal formulae prepared using span 40 and span 60 exhibited excellent flowability while those prepared with span 20 and span 80 showed poor flow properties. TEM photographs revealed that the vesicles were discrete, spherical without aggregation. The mean vesicle size of reconstituted niosomes was found to be in the range between (252.9±0.43–624.3±0.23 nm) with perfect PDI values (0.387±0.05–0.835±0.03). The negative values of zeta potential indicated that all prepared formulae were stabilized by electrostatic repulsion forces. Stability studies confirmed that proniosomes give a more stable system that could overcome the problems of standard niosomes. Formulae with the smallest particle size, higher surface charge values and best flow properties were selected to be loaded with poorly soluble drugs for further study.

Conclusion: The obtained results offered evidence that spray-dried lactose based proniosomes are promising stable drug delivery carriers and ready to incorporate various poorly water-soluble drugs in order to improve their limited oral bioavailability.

Keywords: Proniosomes, Spray dried lactose, Surfactant, Cholesterol, Drug delivery carrier and Bioavailability

DOI: http://dx.doi.org/10.22159/ijap.2018v10i5.27732

INTRODUCTION

Over the decades, the oral route remains the most preferred route of administration for drug delivery. However, a plurality of the new and present drugs taken by oral route usually face bioavailability drawbacks [1]. Different approaches have been employed for improving the dissolution profile of poorly water-soluble drugs [2].

Considerable interest has been focused on the design and formulation of new drug delivery systems. Among them, vesicular drug delivery systems are of high significance. There are different types of vesicular drug delivery systems such as liposomes, niosomes, transferosomes, ethosomes, colloidosomes, and cubosomes. Novel approaches like provesicular drug delivery systems such as proniosomes, layerosomes and ufosomes have also been developed which have higher stabilities compared to conventional and simple vesicular systems [3]. Provesicular systems can be used for prolonged and targeted drug delivery with mild side effects and also provides patient compliance by decreasing the administered dose.

Colloidal particulate drug delivery systems such as liposomes [4] or niosomes [5] are very distinguished in comparison to conventional dosage forms because these vesicular systems can act as drug-containing reservoirs and alter the particle composition or surface to adjust the drug release or the affinity of the drug for the target site. Niosomes are nonionic surfactant vesicles which can entrap both hydrophilic and hydrophobic drugs [6]. Niosomes proved to be an alternative to liposomes because they have more chemical stability and economical as compared to liposomes. But though niosomes reveal good chemical stability, there may be drawbacks of physical instability concerning the dispersions. Similar to liposomes, aqueous niosomal dispersions may show aggregation, fusion, leakage of included drugs, or hydrolysis of encapsulated drugs, thus reducing the shelf life of niosomes [7].

So as to overcome the stability troubles concerning niosomes, proniosomes (dry niosomes) were developed. Proniosomes are dried powder, free flowable, granular product which upon dilution with water develops niosomal dispersion convenient for oral administration [8]. The niosomes formed after reconstitution is analogous to conventional niosomes, however, have uniform size [9].

Different nonionic surfactants with varying HLB were used in the preparation of proniosomes such as polyoxyethylene sorbitan esters (Tweens) [10], polyoxyethylene alkyl ethers (Brijs) and sorbitan esters (spans) [11]. It was noticed that for optimum proniosomes formulations which achieved smaller particle size, and higher entrapment efficiency is obtained within the HLB range from 1 to 8, which is the range of spans [12]. Cholesterol provides rigidity to the niosomes after the hydration of proniosomes and decreases drug leakage, thus increasing the entrapment efficiency. It also stabilizes the structure of the niosomes by inhibition of aggregate formation by exerting steric effect [13].

Different carriers are used in the formation of the dry proniosomes such as: mannitol, sorbitol, lactose and maltodextrin. The desired properties of the carrier include; non-toxicity and *in vivo* safety, poor solubility in the solvent of the loaded solution, free flowability, and excellent water solubility for easy and instant hydration [14]. Spray dried lactose shows optimum behavior as a carrier in proniosomal systems as it has a spherical shape and best flowability among other carriers [15].

There are the various method used for the preparation of proniosomes which include a slurry method and the spraying of

surfactant on solid carrier [16]. There are several factors that must be controlled for the successful formulation of proniosomes. Among the factors, the concentration of surfactant, the ratio of surfactant concentration to cholesterol concentration, the type of the solid carrier and other factors related to the preparation technique such as the amount of organic solvent and the speed of stirring [17].

This research is a screening study aims to prepare plain (unloaded) proniosomes with optimized composition. Factors studied are the surfactant type and the ratio of surfactant to cholesterol. The selection of the optimum proniosomal formula allows a better understanding of the factors that governs the characteristics of the formed niosomes that can be loaded with different drugs. The aim of our work was to assure the feasibility of proniosomes as stable precursors for the development of niosomes as oral drug delivery system for drugs with low oral bioavailability.

MATERIALS AND METHODS

Materials

Cholesterol was purchased from Panreac Quimica SA, Barceolna, Spain. Span 40 (Sorbitan monopalmitate), Span 60 (Sorbitan monostearate) and Sodium Hydroxide were purchased from Oxford Laboratory Chemicals, India. Span 20 (Sorbitan monolaurate) and Span 80 (Sorbitan monooleate) were from Kermel, Chemical Pure, China. Methanol and Chloroform were purchased from Fisons Scientific Equipment, England. Spray Dried Lactose was kindly supplied as a gift sample from Medical Union Pharmaceuticals, Egypt. Sodium Dihydrogen Phosphate was obtained from PureLab, USA. All other chemicals used were of analytical grade.

Methods

Preparation of dry granular proniosomes

Dry Proniosomes were prepared using the slurry method [18]. The composition of various proniosomal formulae is shown in the table (1). Shortly, precisely weighed amounts of lipid mixture (300 µmol) consisting of different grades of spans (20, 40, 60 and 80) and cholesterol at different molar ratios (3:1, 2:1, 1.5:1, 1:1, 1:1.5, 1:2 and 1:3 respectively) were dissolved in 10 ml of solvent mixture containing chloroform and methanol (7:3 ratio). This solution was transferred into a 100 ml round bottomed flask and spray dried lactose (1.5 gm) was added to form slurry [19]. The flask was attached to a rotary evaporator (Heidolph, Germany) and the solvent mixture was evaporated under pressure of 600 mmHg at a temperature of 45±2 °C and 60 rpm until spray dried lactose appeared to be dry as a thin powder film on the flask wall [20]. After ensuring the complete removal of solvent, the resultant powder was scraped and collected. The proniosomal powder was further dried overnight in desiccators at room temperature to obtain dry, free-flowing product. The obtained proniosomal powders were stored in a tightly closed container for further characterization.

Table 1: Compositions of various spray-dried lactose based proniosomal formulae

Formula	Surfactant	Surfactant: cholesterol	Ratio (µmol)	Spray dried lactose (mg)*
F1	Span 20	3:1	225:75	300
F2	Span 20	2:1	200:100	300
F3	Span 20	1.5:1	180:120	300
F4	Span 20	1:1	150:150	300
F5	Span 20	1:1.5	120:180	300
F6	Span 20	1:2	100:200	300
F7	Span 20	1:3	75:225	300
F8	Span 40	3:1	225:75	300
F9	Span 40	2:1	200:100	300
F10	Span 40	1.5:1	180:120	300
F11	Span 40	1:1	150:150	300
F12	Span 40	1:1.5	120:180	300
F13	Span 40	1:2	100:200	300
F14	Span 40	1:3	75:225	300
F15	Span 60	3:1	225:75	300
F16	Span 60	2:1	200:100	300
F17	Span 60	1.5:1	180:120	300
F18	Span 60	1:1	150:150	300
F19	Span 60	1:1.5	120:180	300
F20	Span 60	1:2	100:200	300
F21	Span 60	1:3	75:225	300
F22	Span 80	3:1	225:75	300
F23	Span 80	2:1	200:100	300
F24	Span 80	1.5:1	180:120	300
F25	Span 80	1:1	150:150	300
F26	Span 80	1:1.5	120:180	300
F27	Span 80	1:2	100:200	300
F28	Span 80	1:3	75:225	300

*One milligram of the carrier (spray dried lactose) per 1 µmol of total lipid surfactant mixture.

Evaluation of the proniosomes and proniosome-derived niosomes

Micromeritic properties of powdered proniosomes

The angle of repose (θ)

The angle of repose of powdered proniosomes was measured by the funnel method. Accurately weighed amount was poured through a funnel. The height of the funnel was adjusted accurately in a way that the tip of the funnel just touches the apex of proniosomes powder. The powder was then allowed to flow through the funnel. The radius of the powder pile was measured and the angle of repose determined using the following equation [21]:

$$\tan \theta = h/r$$

Where; h = height of the pile, r = radius of the pile

Bulk and tapped density

Two grams of powdered proniosomes was taken into a 10 ml measuring cylinder. Former volume was observed, and then the cylinder was allowed to fall under its own weight onto a hard flat surface from a height of 2.5 cm at 2-second intervals. The tapping was continued until no change in volume was remarked. Bulk and tapped densities were determined using the following equations [22]:

BD = Powder weight/Bulk Volume

TD = Powder weight/Tapped Volume

Compressibility index

The compressibility of dry proniosomes was calculated by Carr's Index as follow [23]:

Carr's Index (%) = [(TD-BD)/TD] X 100

Hausner ratio

It is the ratio of tapped to bulk density. It provides an idea about the flow properties of the powder and can be determined as follow [24]:

Hausner ratio = TD/BD

Preparation of niosomes from proniosomes and morphological evaluation (Photomicroscopy)

Proniosomes were transformed to noisome by hydrating with 10 ml distilled water at 37 °C and gentle agitation using vortex mixer (MaxiMix II, USA) for 5 min. The formed niosomes were sonicated twice for 30 seconds using sonicator (SONICS VCX 130, USA) [25]. The niosomal dispersion was put on a glass slide, and the formed vesicles were observed at a magnification of 1000x through an optical microscope. The formation of vesicles was observed using an optical microscope and photomicrographs were recorded [26].

Morphological characterization using TEM

The morphology of niosomal dispersion was observed using transmission electron microscopy (JEM-2100, USA). A drop of dispersion was cleaned with phosphate buffer pH 7.4 and put on carbon-coated 300 mesh copper grid and left for 1 minute to form a thin film. These films were then negatively stained with 2% (w/v) phosphotungstic acid solution. After drying with air, the stained films were photographed using TEM [27]. The experiment was performed at room temperature, and micrographs were taken at suitable magnification power.

Analysis of the recorded TEM images

The size distribution of the prepared proniosomes derived niosomes was analyzed using TEM images by the software Nano Measurer 1.2.5 (Fudan University, Shangshai, China) [28].

Particle size analysis and PDI determination

A small amount of freshly prepared proniosomes derived niosomes was used to determine the particle size and PDI. The vesicle size and PDI of the resultant niosomes were measured by dynamic light scattering (DLS) using a photon correlation spectrometer (Zetasizer, Malvern Instruments LTD, UK) which analyzes the fluctuations in light scattering due to the Brownian motion of the particles. Light scattering was monitored at 25 °C at a scattering angle of 90 ° [29].

Zeta potential determination

Zeta potential was determined to measure the stability of reconstituted niosomes. The zeta potential of the formed niosomal dispersions was determined using Zetasizer (Malvern Instruments, UK). Samples were placed in clear disposable zeta cells, and results were noted. Charges on the vesicular surface and their corresponding zeta potential values were obtained [30].

Stability studies

Selected proniosomal formulae were examined for stability by storing them at 4 °C±1 (refrigeration temperature) and at 25 °C±2 (room temperature) for a period of 3 mo [31]. At specific time intervals (0, 30, 60 and 90 d), samples were withdrawn and assessed for micromeritic properties, vesicles size and zeta potential [32].

RESULTS AND DISCUSSION

Evaluation of the proniosomes and proniosome-derived niosomes

Micromeritic properties of powdered proniosomes

Micromeritic properties of proniosomal formulae were considered as an important parameter as it will affect the uniformity of dose and facility of filling into capsules. The flow properties were evaluated with the aid of angle of repose, Carr's index, and Hausner ratio. The angle of repose was found to affect the flowability of the particles. The values less than 20 ° exhibit excellent flowability; the values between 20 and 30 ° show good flowability; the values between 30 and 34 ° exhibit passable flowability; while the values above 34 ° show very poor flowability [33]. Results obtained pointed out that proniosomal formulae containing span 20 [F1, F2, F3, F4, F5, F6 and F7] and span 80 [F22, F23, F24, F25, F26, F27 and F28] which are viscous liquid surfactants have large angle of repose (>30), promising poor flowability. The values obtained for the angle of repose for proniosomal formulae containing span 20 and span 80 ranged from 32.02 °±0.81 to 41.87 °±1.50, as presented in table (2). These values suggest that all proniosomal formulae containing span 20 and span 80 have passable to poor flowability. This may be due to powders cohesivity which affects the flow characteristics and occasionally causes difficulties in powder flow. On the other hand, proniosomal formulae containing span 40 [F8, F9, F10, F11, F12, F13 and F14] and span 60 [F15, F16, F17, F18, F19, F20 and F21] which are solid surfactants have small angle of repose (<30), confirming good flow properties. The values obtained for the angle of repose for proniosomal formulae containing span 40 and span 60 ranged from 24.79°±0.76 to 28.43°±1.30. These values indicate that all proniosomal formulae containing span 40 and span 60 have good flowability.

The flow properties of the prepared proniosomal formulae were also characterized by determining both bulk and tapped densities. From these values, both the Hausner ratio and the Carr's index can be derived. Both bulk and tapped densities were determined with equations described before in the experimental part. These two parameters are related to the flow properties of the prepared powder blend [34]. Carr's index of proniosomal formulae is having span 20 and span 80 was found to be between 21.00±1.32 and 31.38±2.39 indicating poor flowability. However, Carr's index of proniosomal formulae containing span 40 and span 60 ranged between 11.07±2.76 and 19.62±2.50 which give confirmation about the good flow properties of these formulae. These findings were further shored by Hausner ratio values. The Hausner ratio results of proniosomal formulae having span 20 and span 80 were found to be between 1.27±0.02 and 1.46±0.05 indicating poor flowability. On the other hand, proniosomal formulae containing span 40 and span 60 have values of Hausner ratios between 1.13±0.04 and 1.24±0.04 assuring good flow properties. Finally, it was noticed that proniosomal formulae containing span 40 and span 60 have good flow properties. However, those having span 40 and span 60 show poor flowability. This may be due to cohesivity of powders imparted by viscous liquid span 20 and span 80.

Preparation of niosomes from proniosomes and morphological evaluation (Photomicroscopy)

The optical photographs of all reconstituted proniosomal formulae are shown in fig. (1-28). The photographs revealed that the formed niosomes are unilamellar vesicles with a spherical shape and smooth surface. The vesicles were insular and separate without aggregation or lumping. Apparently, proniosomal formulae containing span 40 and span 60 yielded vesicles of large numbers with well-identified outline and core which will affect the entrapment efficiency of loaded drug directly. However proniosomal formulae containing span 20 and span 80 produced small numbers of vesicles with a slightly different outline. This may be due to the high phase transition temperatures of both span 40 and span 60 which will cause the formation of a large number of stable niosomal vesicles. The phase transition temperatures for span 20, 40 and 60 are 16, 42 and 53 °C; respectively, however, span 80 possess the lowest phase transition temperature at 12 °C [35]. This explains why proniosomal formulae containing span 20 and span 80 produce small numbers of vesicles upon hydration.

Table 2: Micromeritic properties of all prepared proniosomal formulae

Formula	Angle of repose*	Bulk density* (g/ml)	Tapped density* (g/ml)	Carr's index* (%)	Hausner ratio*
F1	41.87±1.50	0.5043±0.01	0.6250±0.01	21.00±1.32	1.27±0.02
F2	36.89±1.17	0.5130±0.01	0.6452±0.03	22.23±1.60	1.29±0.03
F3	39.82±1.18	0.5043±0.02	0.6897±0.01	26.05±1.30	1.35±0.02
F4	36.20±0.57	0.5311±0.01	0.7407±0.02	27.43±1.36	1.38±0.03
F5	36.87±0.60	0.5173±0.01	0.7143±0.01	25.84±2.27	1.35±0.04
F6	33.99±0.52	0.5043±0.01	0.6897±0.01	25.19±2.22	1.34±0.04
F7	32.02±0.81	0.5218±0.01	0.6897±0.01	26.07±2.27	1.35±0.04
F8	28.43±1.30	0.4919±0.02	0.5714±0.01	13.11±1.33	1.15±0.02
F9	28.20±0.97	0.5043±0.01	0.5882±0.01	12.61±0.19	1.14±0.01
F10	27.17±1.01	0.5000±0.01	0.5882±0.02	15.00±2.50	1.18±0.03
F11	26.21±0.86	0.4959±0.01	0.5714±0.01	12.38±2.32	1.14±0.03
F12	27.77±0.62	0.5085±0.01	0.6061±0.01	16.94±1.37	1.20±0.02
F13	25.13±0.80	0.5130±0.02	0.6452±0.01	19.62±2.50	1.24±0.04
F14	26.01±0.55	0.4959±0.01	0.6061±0.02	14.88±2.51	1.18±0.03
F15	26.39±0.86	0.4959±0.01	0.5882±0.01	16.50±2.61	1.20±0.04
F16	27.16±0.60	0.5043±0.01	0.5882±0.01	15.94±2.70	1.19±0.04
F17	25.12±0.59	0.5173±0.01	0.5714±0.01	11.18±2.84	1.13±0.04
F18	28.20±0.97	0.4959±0.01	0.5714±0.01	12.38±2.32	1.14±0.03
F19	25.87±1.36	0.5002±0.01	0.5882±0.02	14.98±2.36	1.18±0.03
F20	24.79±0.76	0.5130±0.01	0.5714±0.01	11.07±2.76	1.13±0.03
F21	26.21±0.86	0.4919±0.01	0.5882±0.01	18.03±1.30	1.22±0.02
F22	39.08±1.76	0.4959±0.01	0.7143±0.02	31.38±2.39	1.46±0.05
F23	39.42±0.66	0.5130±0.01	0.6897±0.01	26.49±0.94	1.36±0.02
F24	37.58±1.07	0.5043±0.01	0.6897±0.03	30.26±2.54	1.44±0.05
F25	34.02±1.38	0.5173±0.01	0.6897±0.01	24.13±1.34	1.32±0.02
F26	36.54±1.01	0.5000±0.01	0.6667±0.01	23.33±1.44	1.30±0.02
F27	34.92±1.07	0.5085±0.01	0.6250±0.02	21.15±1.57	1.27±0.06
F28	35.25±1.44	0.5218±0.01	0.6897±0.01	24.34±1.13	1.32±0.02

*Results are expressed as mean±S. D, n=3

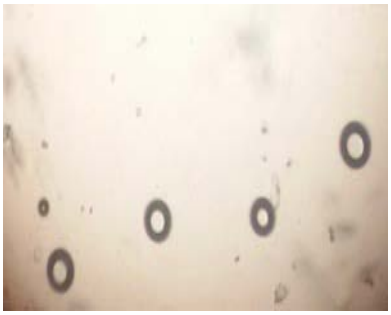

Fig. 1: Optical photograph of F1

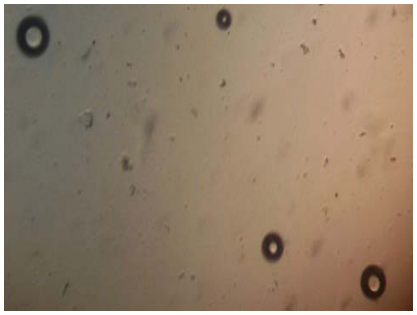

Fig. 2: Optical photograph of F2

Fig. 3: Optical photograph of F3

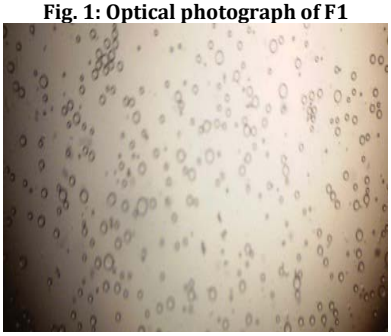

Fig. 4: Optical photograph of F4

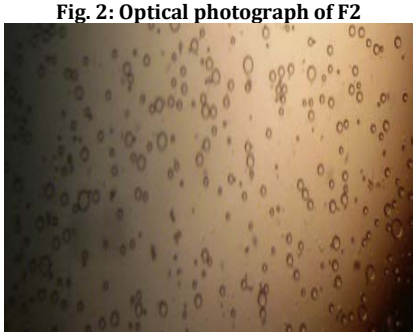

Fig. 5: Optical photograph of F5

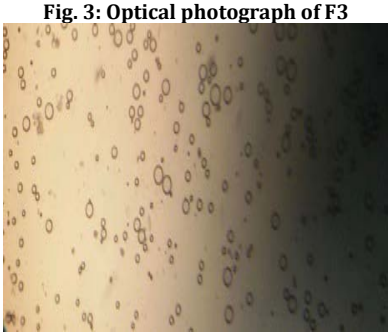

Fig. 6: Optical photograph of F6

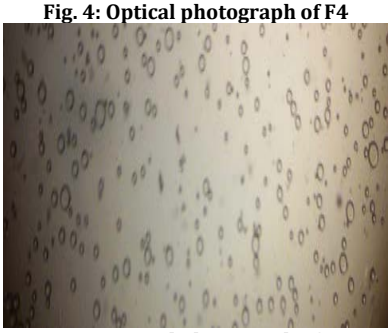

Fig. 7: Optical photograph of F7

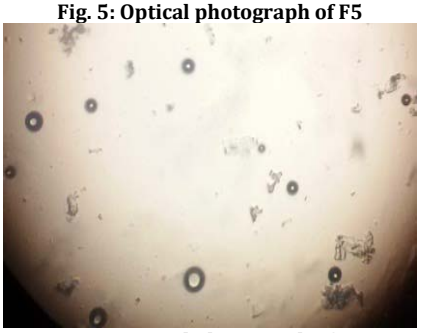

Fig. 8: Optical photograph of F8

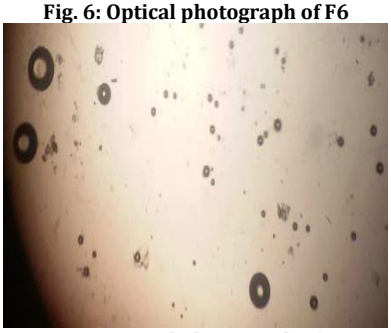

Fig. 9: Optical photograph of F9

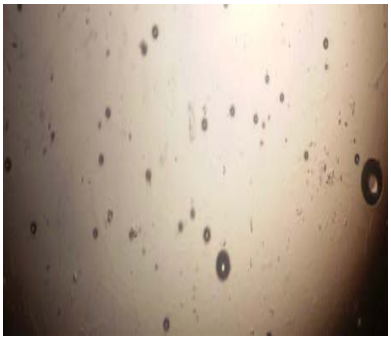
Fig. 10: Optical photograph of F10

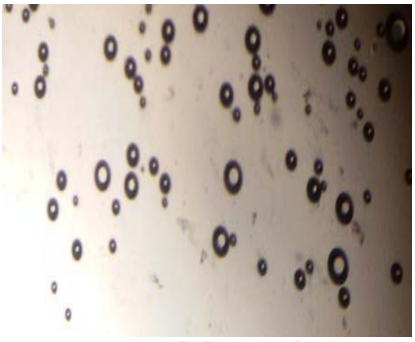
Fig. 11: Optical photograph of F11

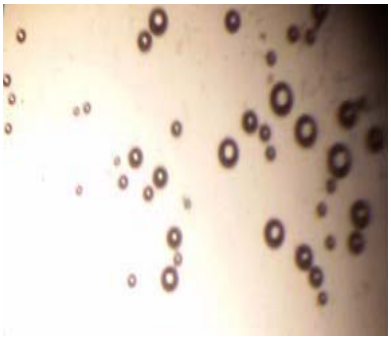
Fig. 12: Optical photograph of F12

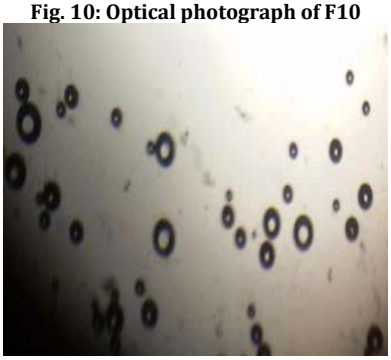
Fig. 13: Optical photograph of F13

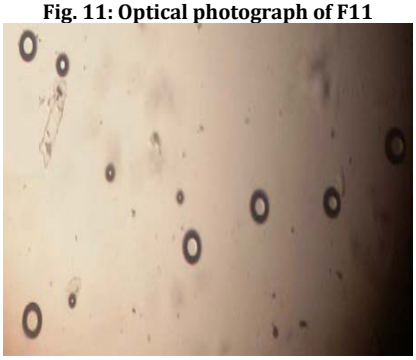
Fig. 14: Optical photograph of F14

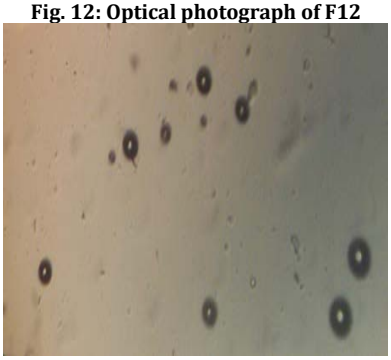
Fig. 15: Optical photograph of F15

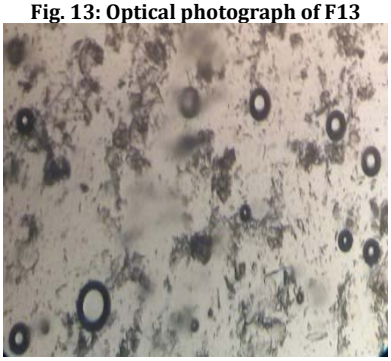
Fig. 16: Optical photograph of F16

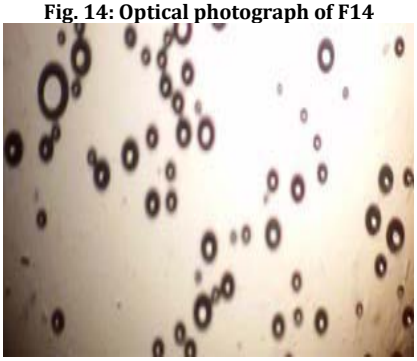
Fig. 17: Optical photograph of F17

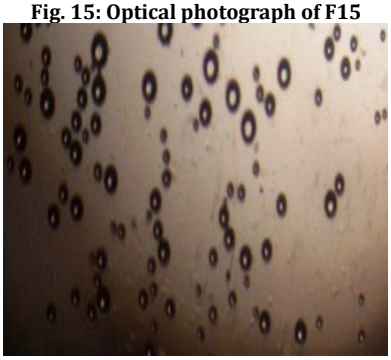
Fig. 18: Optical photograph of F18

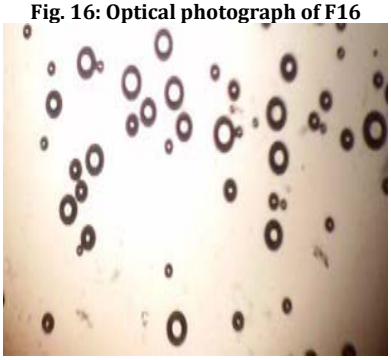
Fig. 19: Optical photograph of F19

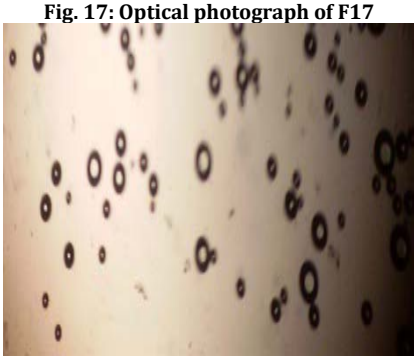
Fig. 20: Optical photograph of F20

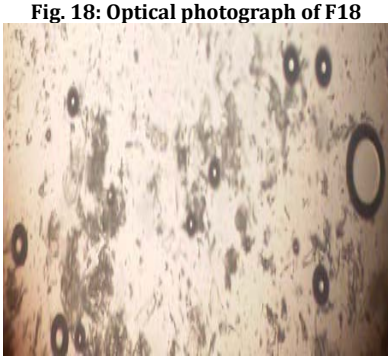
Fig. 21: Optical photograph of F21

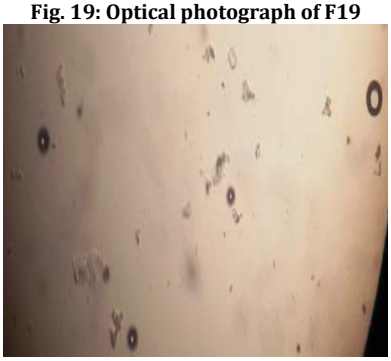
Fig. 22: Optical photograph of F22


Fig. 23: Optical photograph of F23


Fig. 24: Optical photograph of F24

Fig. 25: Optical photograph of F25

Fig. 26: Optical photograph of F26

Fig. 27: Optical photograph of F27

Fig. 28: Optical photograph of F28

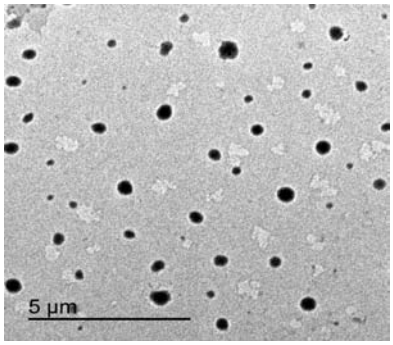

Fig. 29: TEM photograph of F1

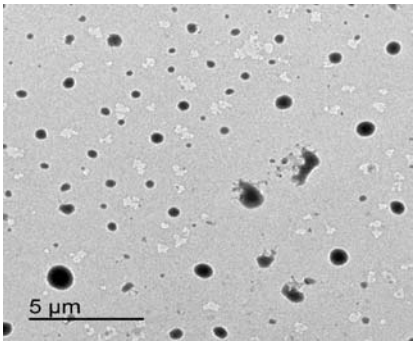

Fig. 30: TEM photograph of F2

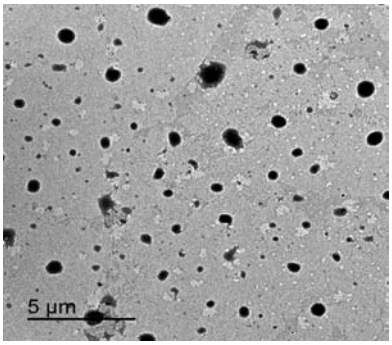

Fig. 31: TEM photograph of F3

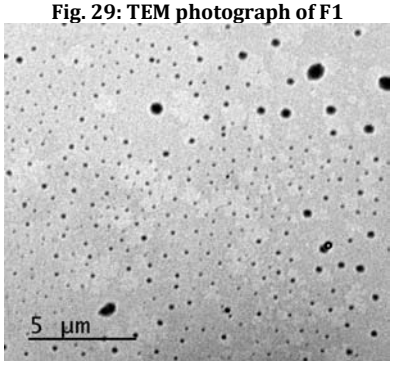

Fig. 32: TEM photograph of F4

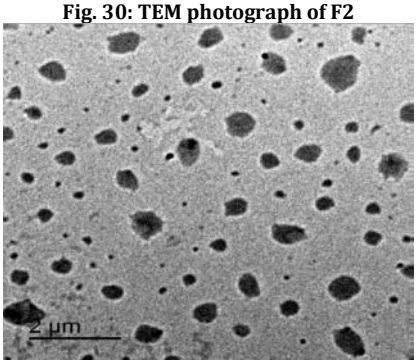

Fig. 33: TEM photograph of F5

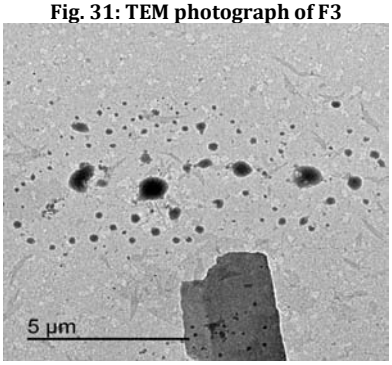

Fig. 34: TEM photograph of F6

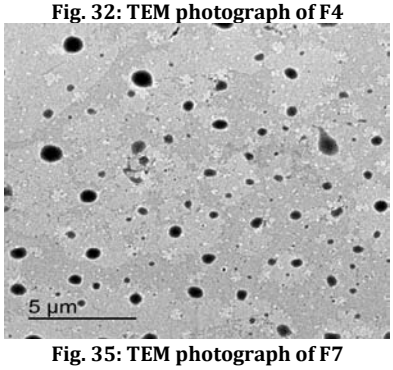

Fig. 35: TEM photograph of F7

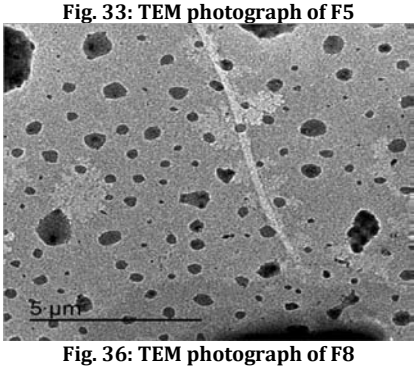

Fig. 36: TEM photograph of F8

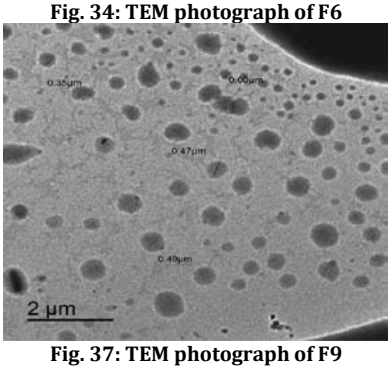

Fig. 37: TEM photograph of F9

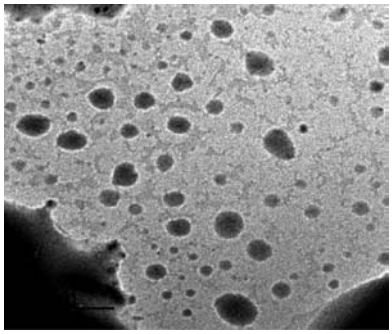

Fig. 38: TEM photograph of F10

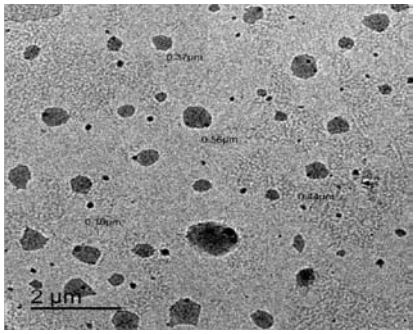

Fig. 39: TEM photograph of F11

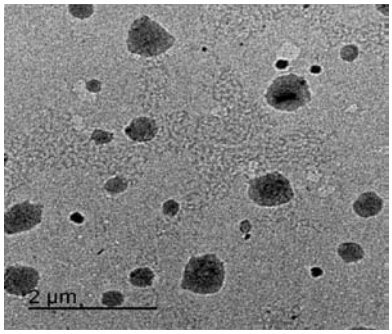

Fig. 40: TEM photograph of F12

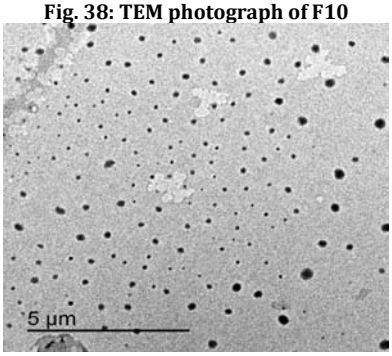

Fig. 41: TEM photograph of F13

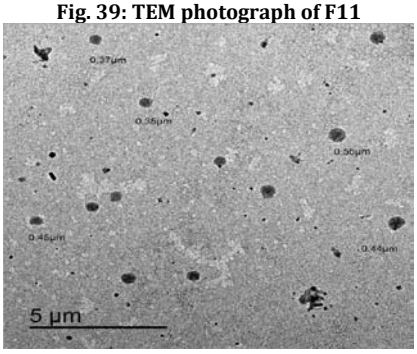

Fig. 42: TEM photograph of F14

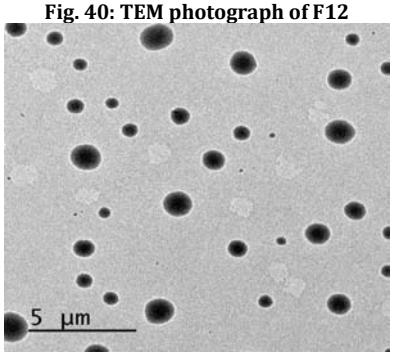

Fig. 43: TEM photograph of F15

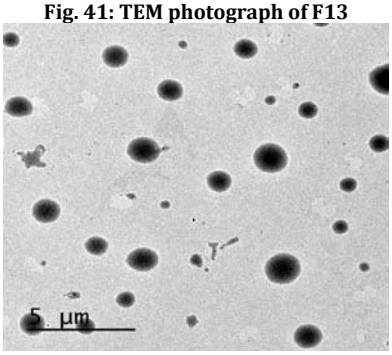

Fig. 44: TEM photograph of F16

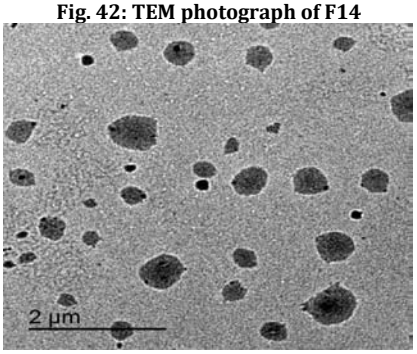

Fig. 45: TEM photograph of F17

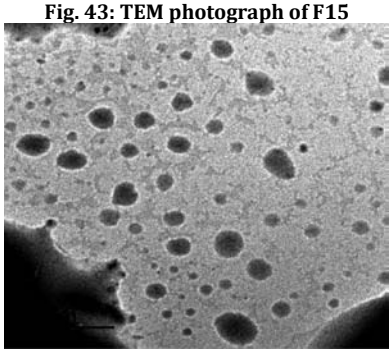

Fig. 46: TEM photograph of F18

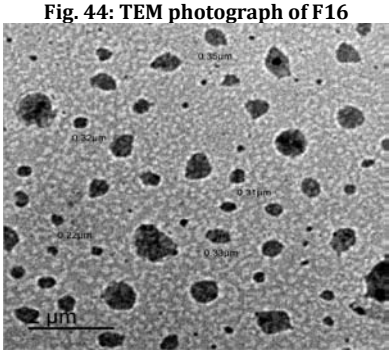

Fig. 47: TEM photograph of F19

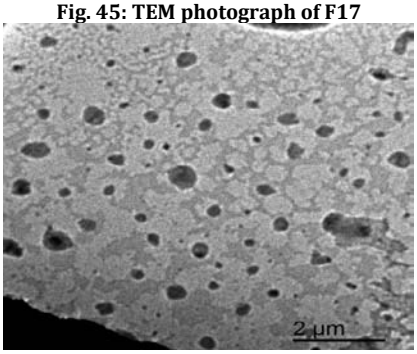

Fig. 48: TEM photograph of F20

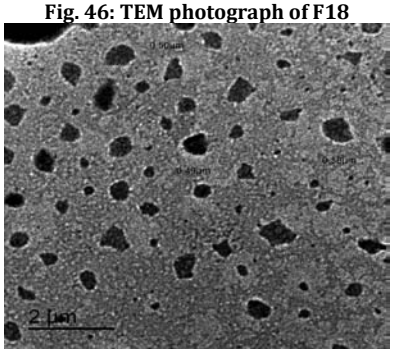

Fig. 49: TEM photograph of F21

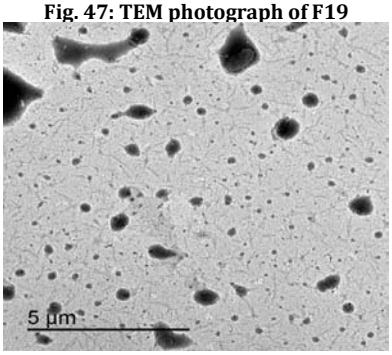

Fig. 50: TEM photograph of F22

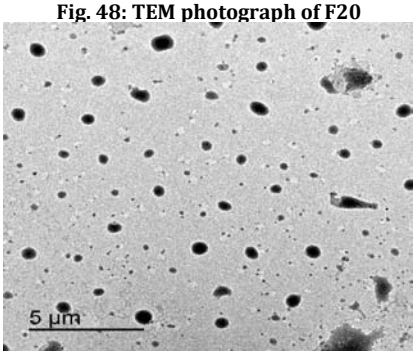

Fig. 51: TEM photograph of F23

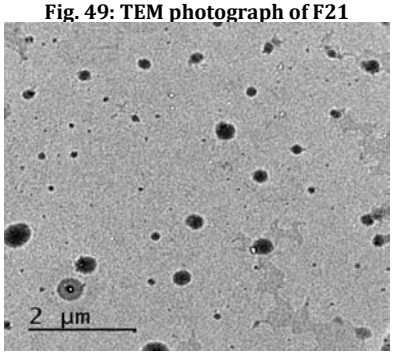

Fig. 52: TEM photograph of F24

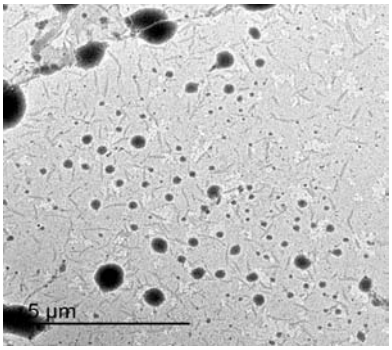

Fig. 53: TEM photograph of F25

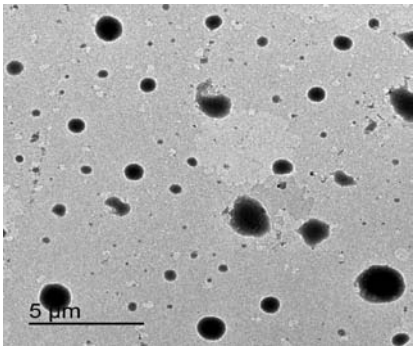

Fig. 54: TEM photograph of F26

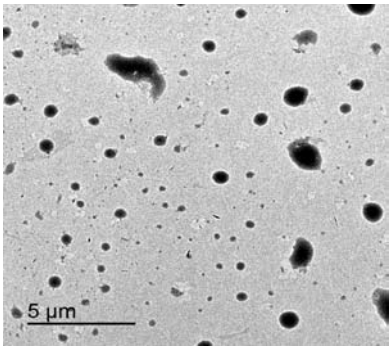

Fig. 55: TEM photograph of F27

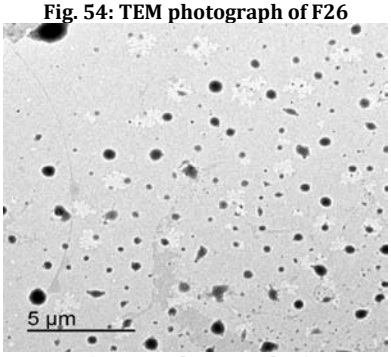

Fig. 56: TEM photograph of F28

Morphological characterization using TEM

Vesicles formation was further confirmed by TEM. The transmission electron microscopy photographs of the niosomes prepared from proniosomal formulae are shown in fig. (29-56). From the presented figures, it is apparent that the majority of the vesicles are well identified, nanosized and separate with sharp outermost bilayer boundaries having large internal space. The vesicles seem to be like a spherical reservoir and devoid of any surface artifacts.

Analysis of the recorded TEM images

Analysis of TEM photographs of all proniosomal formulae using the software Nano Measurer 1.2.5 revealed that the mean particle size of all prepared formulae ranged between 142.98 nm (F13) and 861.98 nm (F15) as presented in fig. (57-84). The discussion of particle size analysis results here is illogical as TEM images represent a very small section of the sample so full discussion of particle size analysis will be in the next test. We just took an overview about particle size distribution of all prepared formulae.

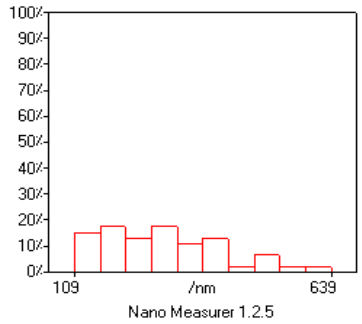

Fig. 57: Size distribution of F1

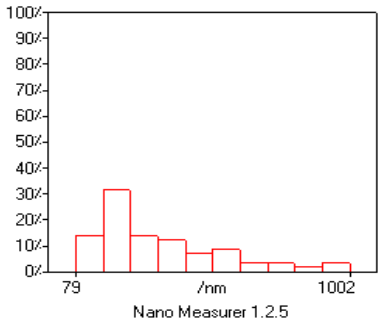

Fig. 58: Size distribution of F2

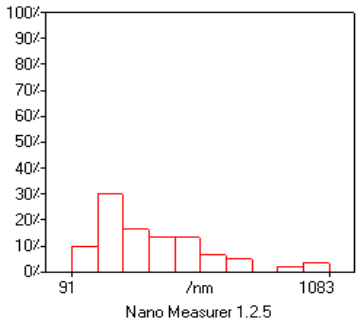

Fig. 59: Size distribution of F3

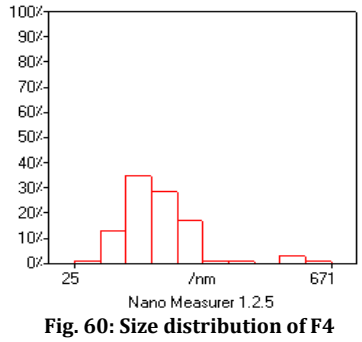

Fig. 60: Size distribution of F4

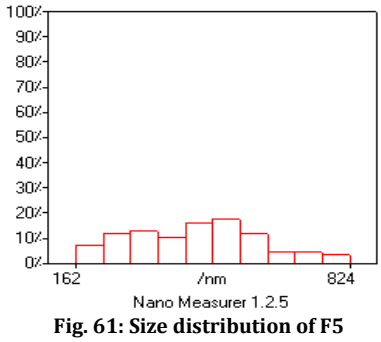

Fig. 61: Size distribution of F5

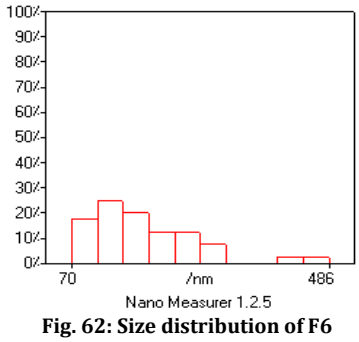

Fig. 62: Size distribution of F6

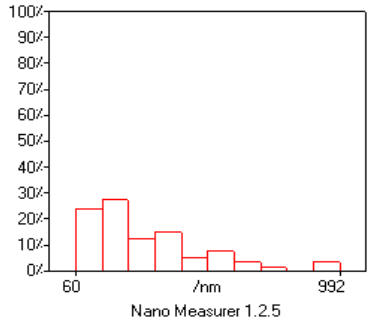

Fig. 63: Size distribution of F7

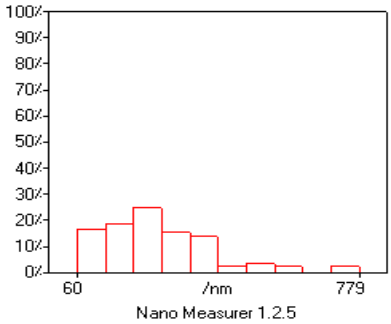

Fig. 64: Size distribution of F8

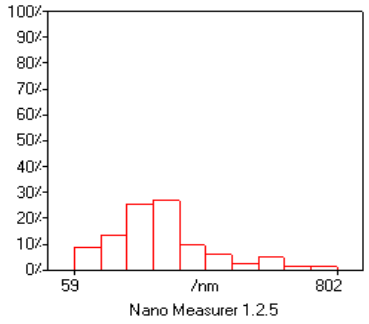

Fig. 65: Size distribution of F9

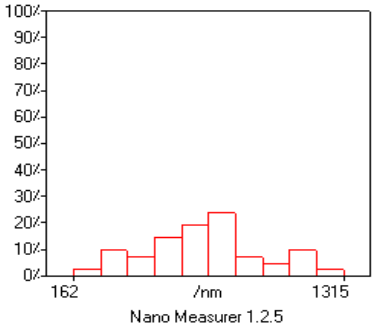

Fig. 66: Size distribution of F10

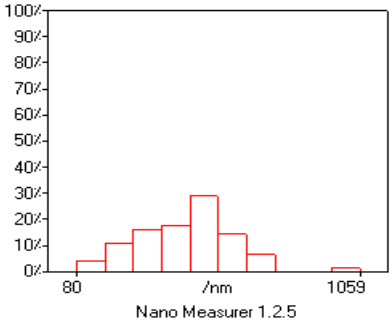

Fig. 67: Size distribution of F11

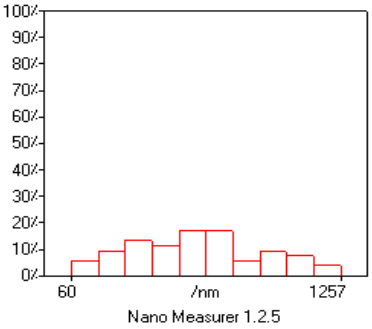

Fig. 68: Size distribution of F12

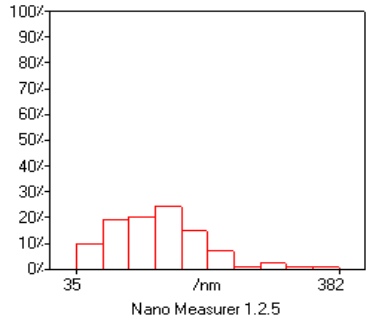

Fig. 69: Size distribution of F13

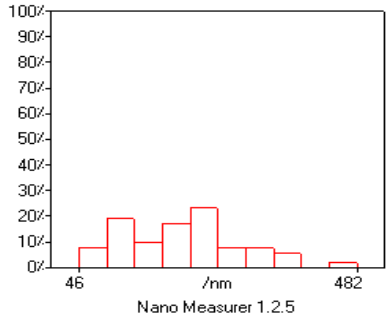

Fig. 70: Size distribution of F14

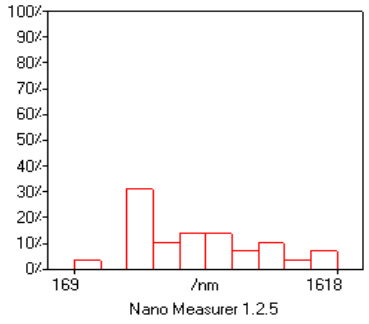

Fig. 71: Size distribution of F15

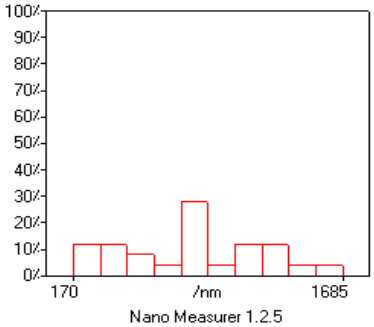

Fig. 72: Size distribution of F16

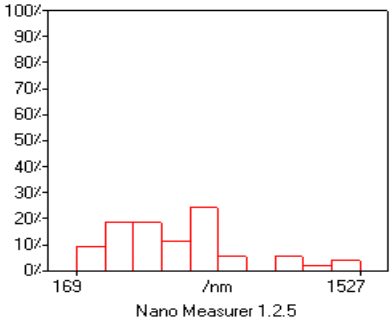

Fig. 73: Size distribution of F17

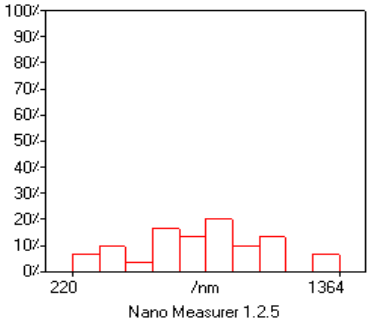

Fig. 74: Size distribution of F18

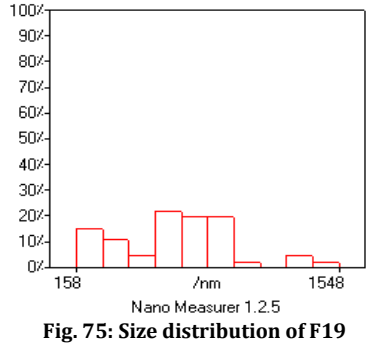

Fig. 75: Size distribution of F19

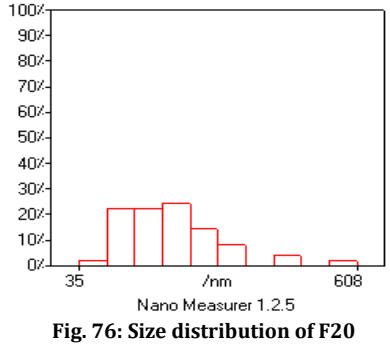

Fig. 76: Size distribution of F20

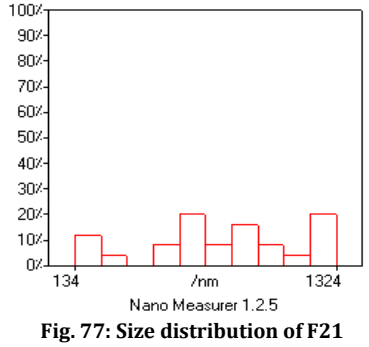

Fig. 77: Size distribution of F21

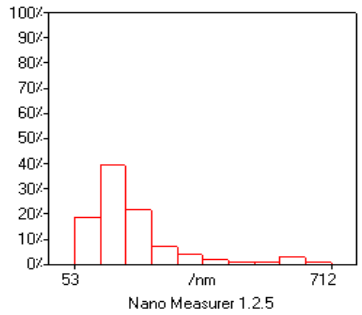

Fig. 78: Size distribution of F22

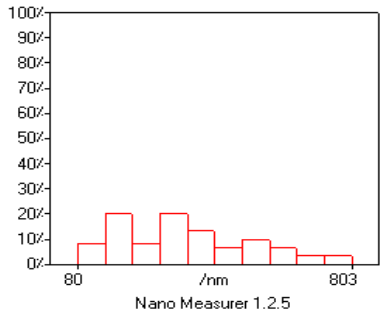

Fig. 79: Size distribution of F23

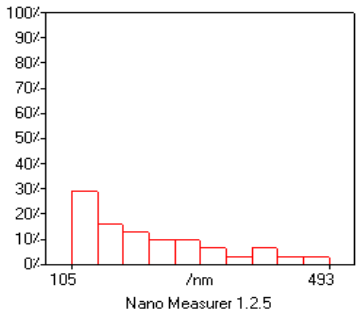

Fig. 80: Size distribution of F24

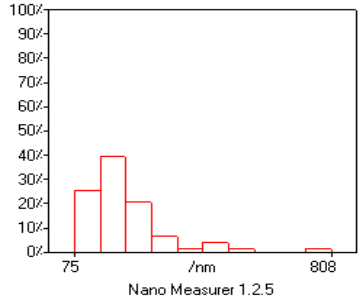

Fig. 81: Size distribution of F25

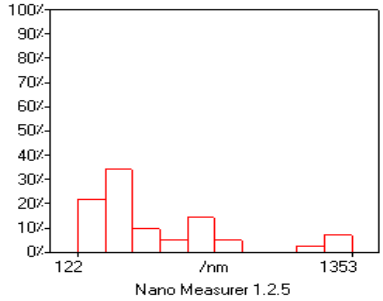

Fig. 82: Size distribution of F26

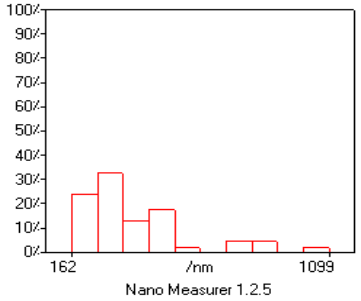

Fig. 83: Size distribution of F27

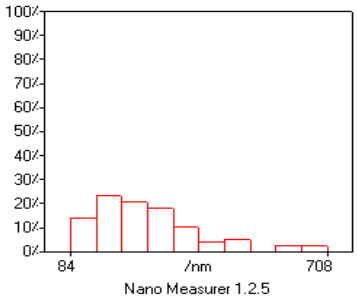

Fig. 84: Size distribution of F28

Particle size analysis and PDI determination

Vesicles size and particle size distribution are important parameters for the vesicular drug delivery systems. The particle size of the formed vesicles was in the nanometric dimensions ranging from 252.9±0.43 nm (F4) to 624.3±0.23 nm (F28) as seen in the table (3). From the particle size analysis, it was clear that there are two factors affecting particle size which are surfactant type and cholesterol content. There was an increment in the vesicular size upon increasing the alkyl chain length of surfactant. The size of the vesicles increased gradually from span 20 (252.9±0.43–357.2±0.56 nm) <span 40 (361.7±0.84–419.1±1.05 nm) <span 60 (428.2±0.74–494.6±0.51 nm)<span 80 (512.4±0.47-624.3±0.23 nm). This increment is linked to the alkyl chain length of span (C12-C18), which leads to elevated critical packing parameter thus the vesicle size increases [36]. It was also observed as the cholesterol concentration increased, an increase in the mean vesicle size occurred. This comes in accordance with the research done by Manconi *et al.* [37], who noted that, as the cholesterol surfactant ratio decreased in niosomal formulae, reduction in the vesicle size occur. The structure properties of cholesterol and its lipid solubility are the cause for its effect on the vesicle size. Cholestrol is loaded in hollow spaces between the surfactant molecules and expands the vesicles bilayers thus increased the particle size of vesicles [38]. It was also noticed that small sized vesicles with high surface charge values formed when the equal molar ratio of surfactant and cholesterol were used as presented in table (3). Our results also comply with the literature reports [39]. The mean particle size is not the only parameter to be considered in the formulation of proniosomes. The size distribution is another parameter of equal importance. The polydispersity index was calculated according to Bhavana *et al.* [40]. A polydispersity index of 1 indicates large variations in particle size; a reported value of 0 means that size variation is absent [41]. The obtained low PDI values of all proniosomes derived niosomes (0.387±0.05–0.835±0.03) indicate a limited variation in particle size as reported in the table (3).

Zeta potential determination

Zeta potential predicts the stability of the carrier system. The higher the zeta potential value, the more repulsion between charged particles and hence the more stability against aggregation. Particles with zeta potential values more than (+30 mV) or less than (-30 mV) are considered stable [42]. The zeta potential values of all prepared proniosomal formulae are listed in table (3). The values ranged from between-18.3±0.56 to-43.8±0.35 mV which are high enough for electrostatic stabilization. Negative values of all prepared formulae indicate the formation of stable systems [43]. This higher charge on the vesicle surfaces produces a repulsion force which made them stable, devoid of aggregation and providing an evenly distributed dispersion. These results were in complete accordance with Litha *et al.* who prepared Clotrimazole based proniosomes, and found that zeta potential of the optimized formula was-44.45 mV [44].

Stability studies

Based upon the rank order employed for all proniosomal formulae depending on their characterization, two optimized proniosomal formulae were selected to be tested for stability study. From the particle size analysis, zeta potential and micromeritic properties, formulae F11 and F9 were chosen respectively as illustrated in table (4). The physical appearance, micromeritic properties, vesicle size and zeta potential were monitored for the optimized proniosomal

powder formulae F9 and F11 upon storage at refrigerated and ambient room temperature for a period of 90 d as shown in the table (5). The results indicated that there was no appreciable change in physical appearance, flow characteristics and zeta potential when formulae F9 and F11 were stored at refrigerated and room temperatures. However, there was a slight increase in vesicle size of the prepared formulae. This increase was higher in formulae stored at room temperature than at refrigerated temperature indicating that prepared formulae were relatively stable at 4±1 °C, as compared to 25 °C±2. The stability studies suggest that the proniosomal formulae were comparatively more stable when stored at refrigerated conditions compared to room temperature.

Table 3: Particle size, PDI and zeta potential of all prepared proniosomal formulae

Formula	Particle size* (nm)	PDI*	Zeta potential* (mV)
F1	308.0±0.25	0.387±0.05	-40.4±0.87
F2	298.8±0.74	0.835±0.03	-40.8±1.17
F3	264.6±0.50	0.505±0.08	-41.2±0.45
F4	252.9±0.43	0.591±0.11	-42.3±0.71
F5	330.3±0.14	0.432±0.19	-39.0±0.09
F6	357.2±0.56	0.477±0.04	-36.4±0.24
F7	338.2±0.33	0.596±0.02	-28.4±0.17
F8	366.8±0.61	0.610±0.14	-41.4±0.61
F9	365.9±0.17	0.411±0.02	-43.8±0.35
F10	361.7±0.84	0.626±0.09	-43.4±0.26
F11	396.9±1.14	0.431±0.06	-41.4±0.44
F12	410.4±0.27	0.444±0.04	-42.6±1.12
F13	386.7±0.83	0.678±0.05	-39.0±0.28
F14	419.1±1.05	0.403±0.12	-39.5±0.33
F15	448.3±0.44	0.433±0.07	-30.3±0.49
F16	433.9±0.65	0.605±0.14	-22.2±0.39
F17	446.8±0.37	0.410±0.16	-38.4±0.75
F18	428.2±0.74	0.416±0.08	-28.6±0.14
F19	455.5±0.41	0.460±0.06	-24.3±0.42
F20	494.6±0.58	0.652±0.20	-22.1±0.39
F21	470.8±0.29	0.409±0.04	-23.1±1.04
F22	512.4±0.47	0.630±0.13	-18.3±0.56
F23	554.5±0.95	0.469±0.07	-24.6±0.27
F24	541.8±0.71	0.487±0.11	-36.9±0.08
F25	518.7±0.18	0.478±0.08	-22.0±0.15
F26	558.7±0.53	0.526±0.09	-24.6±0.47
F27	622.0±0.88	0.540±0.14	-23.1±1.09
F28	624.3±0.23	0.512±0.03	-24.5±0.24

*Results are expressed as mean±SD, n=3

Table 4: Rank order of all proniosomal formulae according to particle size analysis, zeta potential and micromeritic properties

Formula	Particle Size	Zeta potential	Angle of repose	Hausner ratio	Total rank order	Conclusive rank order
F1	4	1	28	15	48	10
F2	3	9	23	17	52	12
F3	2	8	27	23	60	17
F4	1	5	20	26	52	12
F5	5	11	22	22	60	17
F6	7	15	16	21	59	16
F7	6	18	15	24	63	21
F8	10	6	14	6	36	5
F9	9	2	12	5	28	**2**
F10	8	3	10	8	29	3
F11	12	6	6	3	27	**1**
F12	13	4	11	12	40	8
F13	11	11	3	14	39	7
F14	14	10	5	7	36	5
F15	18	16	8	11	53	14
F16	16	25	9	10	60	17
F17	17	13	2	2	34	4
F18	15	17	12	3	47	9
F19	19	22	4	8	53	14
F20	21	26	1	1	49	11
F21	20	23	6	13	62	20
F22	22	28	25	28	103	28
F23	25	19	26	25	95	27
F24	24	14	24	27	89	26
F25	23	27	17	19	86	24
F26	26	19	21	18	84	22
F27	27	23	18	16	84	22
F28	28	21	19	20	88	25

Table 5: Effect of storage on micromeritic properties, vesicle size and zeta potential of proniosomal formulae F9 and F11 at room and refrigeration temperatures

	Time (Day)	F9		F11	
		4 °C	25 °C	4 °C	25 °C
Angle of repose*	0	27.34±0.71		26.69±0.24	
	30	28.87±0.33	27.11±0.58	26.47±0.67	27.18±0.89
	60	28.55±0.94	28.68±0.24	28.35±0.38	30.87±0.08
	90	27.39±0.57	30.22±0.84	27.59±0.42	32.15±0.14
Carr's index* (%)	0	13.24±1.04		12.81±0.81	
	30	14.74±0.61	13.87±1.29	14.55±0.72	13.31±0.48
	60	13.08±0.37	15.49±0.78	14.17±0.35	15.94±0.15
	90	13.54±0.88	17.32±0.26	13.31±0.41	16.28±1.14
Hausner ratio*	0	1.20±		1.19±	
	30	1.21±0.06	1.22±0.04	1.22±0.02	1.18±0.01
	60	1.14±0.09	1.24±0.06	1.18±0.05	1.21±0.05
	90	1.18±0.02	1.27±0.03	1.17±0.01	1.24±0.07
Vesicle size* (nm)	0	320.70±1.94		375.84±2.04	
	30	335±1.23	357±2.14	394±1.22	438±0.87
	60	327±0.84	384±0.53	405±2.37	429±1.69
	90	348±1.57	387±0.71	416±1.90	433±2.08
Zeta potential* (mV)	0	-42.7±0.64		-40.1±1.23	
	30	-40.5±1.06	-39.5±0.32	-41.5±0.29	-39.4±0.58
	60	-41.3±0.48	-40.7±1.29	-40.3±0.67	-35.3±1.84
	90	-38.2±1.59	-36.4±0.81	-40.7±1.39	-37.7±0.79

*Results are expressed as mean±SD, n=3

CONCLUSION

The unloaded prepared vesicular systems were found to fulfill the characteristics of proniosomes. They had a particle size in the nanometric range, negative high zeta potential values as well as good flow characters. The optimized proniosomal formula containing span 40 and cholesterol in equimolar ratio exhibited low size, high surface charge, and good flow properties. The obtained results offered evidence that spray-dried lactose based proniosomes are promising stable drug delivery carriers and ready to incorporate different poorly water-soluble drugs in order to improve their limited oral bioavailability.

AUTHORS CONTRIBUTIONS

All the author have contributed equally

CONFLICTS OF INTERESTS

The authors declare no conflict of interest

REFERENCES

1. Ghorab M, Elsayed M, Nasr A, Gad S. Effect of additives on *in vitro* release of the orodispersible dosage form. Int J Pharm Pharm Sci 2015;7:283-9.
2. Dizaj S, Vazifehasl Z, Salatin S, Adibkia K, Javadzadeh Y. Nanosizing of drugs: effect on dissolution rate. Res Pharm Sci 2015;10:95-108.
3. Bayindir Z, Yuksel N. Provesicles as novel drug delivery systems. Curr Pharm Biotechnol 2015;16:344-64.
4. Couvreur P, Fattal E, Andremont A. Liposomes and nanoparticles in the treatment of intracellular bacterial infections. Pharm Res 1991;8:1079-86.
5. Schreier H, Bouwstra J. Liposomes, and niosomes as topical drug carriers: dermal and transdermal drug delivery. J Controlled Release 1994;30:1-15.
6. Gannu P, Pojaku R. Nonionic surfactant vesicular systems for effective drug delivery-an overview. Acta Pharm Sin B 2011;1:208-19.
7. Krishnagopal D, Alpana R. Niosome as a novel drug delivery system-a review. Int J Appl Pharm 2013;6:1-7.
8. Sunil K, Pushpendra K, Nalini P, Gyanendra Saxena. Comparative study of proniosomal drug delivery system of flurbiprofen. J Chem Pharm Res 2016;8:222-8.
9. Ye J, Jingyuan W, Sanjay G, Da L, Yulin Z, Lirong T, *et al*. Development of a novel niosomal system for oral delivery of Ginkgo biloba extract. Int J Nanomed 2013;8:421-30.
10. Peeyush V, Alpana R. Non-ionic provesicular drug carrier: an overview. Asian J Pharm Clin Res 2013;6:38-42.
11. Karim M, Asim S, Nikhil B, Arijit G, Sugata C, Mamata Behera, *et al*. Niosome: a future of targeted drug delivery systems. J Adv Pharm Technol Res 2010;1:374-80.
12. Zerrin S, Nilufer Y. Investigation of formulation variables and excipient Interaction on the production of Niosomes. AAPS PharmSciTech 2012;13:826-35.
13. Okore V, Attama A, Ofokansi K, Esimone C, Onuigbo E. Formulation and evaluation of Niosomes. Indian J Pharm Sci 2011;73:323-8.
14. Radha G, Sudha R, Sarvani B. A review on proniosomal drug delivery system for targeted drug action. J Basic Clin Pharm 2013;4:42-8.
15. Abd-Elbary A, El-laithy H, Tadros M. Sucrose stearate-based proniosome-derived niosomes for the nebulisable delivery of cromolyn sodium. Int J Pharm 2008;357:189-98.
16. Almira I, David G. Maltodextrin-based proniosomes. AAPS PharmSci 2001;3:1-8.
17. Vajihe A, Daryoush A, Abbas P, Hojjat S. Release studies on ciprofloxacin loaded non-ionic surfactant vesicles. Avicenna J Med Biotechnol 2015;7:69-75.
18. Gurrapu A, Jukanti R, Reddy S, Kanuganti S, Jeevana J. Improved oral delivery of valsartan from maltodextrin based proniosome powders. Adv Powder Technol 2012;3:583-90.
19. Jigar V, Puja V, Krutika S. Formulation and evaluation of topical niosomal gel of erythromycin. Int J Pharm Pharm Sci 2011;3:123-6.
20. Tank C, Borkhataria C, Baria A. Formulation and evaluation of aceclofenac loaded maltodextrin based proniosomes. Int J ChemTech Res 2009;1:567-73.
21. Sajeev C, Vinay G, Archna R, Saha R. Oral controlled release formulation of diclofenac sodium by microencapsulation with ethylcellulose. J Microencap 2002;19:753-60.
22. Bhagwat A, D`Souza I. Formulation and evaluation of solid SMEDDS using aerosil 200 as solid carrier. Int Curr Pharm J 2012;12:414-9.
23. Surender R, Mahalaxmi R, Srinivas P, Deepak K, Kumar A, Sneh P. Self-emulsifying systems of Aceclofenac by extrusion/Spheronization: formulation and evaluation. J Chem Pharm Res 2011;3:280-9.
24. Veerareddy P, Bobbala S. Enhanced oral bioavailability of isradipine via proniosomal systems. Drug Dev Ind Pharm 2013;39:909-17.
25. Dalia S, Mohamed N, Mirhan M. Bioavailability and hypo-cholesterolemic effect of proniosomal simvastatin for transdermal delivery. Int J Pharm Pharm Sci 2013;5:344-51.
26. Preethy C, Boby J, Noby T, Praveen R, Jeny S, Betty C. Formulation and characterization of maltodextrin based

proniosomes of cephalosporins. World J Pharm Sci 2015;3:62-74.

27. Nasr A, Gardouh A, Ghonaim H, Abdelghany E, Ghorab M. Effect of oils, surfactants and cosurfactant on phase behavior and physicochemical properties of self-nanoemulsifying drug delivery system (SNEDDS) for irbesartan and olmesartan. Int J Appl Pharm 2016;8:13-24.
28. Bitao F, Shujun C, Qiufang Y, Qingfeng S, Chunde J. Fabrication of cellulose nanofiber/AlOOH aerogel for flame retardant and thermal insulation. Materials 2017;10:1-10.
29. Mehanna M, Elmaradny H, Samaha M. Mucoadhesive liposomes as ocular delivery system: physical, microbiological, and *in vivo* assessment. Drug Dev Ind Pharm 2010;36:108-18.
30. Meenakshi K, Parvat K, Ashwani S, Divya D, Mayank K, Nidhi S. Formulation, characterization and *in vitro* evaluation of tactically engineered proniosomes for successful oral delivery of ramipril. Pharm Lett 2015;7:93-7.
31. Jadon P, Gajbhiye V, Jadon R. Enhanced oral bioavailability of griseofulvin via niosomes. AAPS PharmSciTech 2009;10:1186-92.
32. Hao Y, Zhao F, Li N, Yang Y. Studies on a high encapsulation of colchicine by niosome system. Int J Pharm 2002;244:73-80.
33. Bhowmik D, Chiranjib B, Krishnakanth S, Pankaj R, Chandira M. Fast dissolving tablet. J Chem Pharm Res 2009;1:163-77.
34. Sahoo S, Mallick A, Barik B, Senapati P. Preparation and in vitro evaluation of ethylcellulose microspheres containing stavudine by the double emulsion method. Die Pharmazie 2007;62:117-21.
35. Somayeh T, Jaleh V. Effect of different types of surfactants on the physical properties and stability of carvedilol nano-niosomes. Adv Biomed Res 2016;5:1-6.
36. Uchegbu I, Florence A. Non-ionic surfactant vesicles (niosomes): physical and pharmaceutical chemistry. Adv Colloid Interface Sci 1995;58:1-55.
37. Manconi M, Sinico C, Valenti D, Fadda A. Niosomes as carriers for tretinoin. I. preparation and properties. Int J Pharm 2002;234:237-48.
38. Al-Muhammed J, Ozer A, Ercan M, Hincal A. *In vivo* studies on dexamethasone sodium phosphate liposomes. J Microencapsul 1996;13:293-306.
39. Gopinath D, Ravi D, Rao B, Apte S, Renuka D, Rambhau D. Ascorbyl palmitate vesicles (Aspasomes): formation, characterization and applications. Int J Pharm 2004;271:95-113.
40. Bhavana V, Ajay J, Jain N. Proniosome based transdermal delivery of levonorgestrel for effective contraception. J Controlled Release 1998;54:149-65.
41. Raymond M, Josbert M, Marcel H, Adrienne P, Grietje M, Gert S. Liposome-encapsulated prednisolone phosphate inhibits growth of established tumors in mice. Neoplasia 2005;7:118-27.
42. Hanaor D, Michelazzi M, Leonelli C, Sorrell C. The effects of carboxylic acids on the aqueous dispersion and electrophoretic deposition of ZrO_2. J Eur Ceram Soc 2012;32:235-44.
43. Rai S, Yasir M. Preparation, optimization and *in vitro* evaluation of cinnarizine loaded lipid based system. IOSR J Pharm 2012;2:47-56.
44. Litha T, Vidya V. Formulation and optimization of clotrimazole loaded proniosomal gel using 3^2 factorial design. Sci Pharm 2012;80:731-48.